The Resistance of the Septum of the Median Giant Axon of the Earthworm

PETER BRINK and LLOYD BARR

From the Department of Physiology and Biophysics, University of Illinois, Urbana, Illinois, 61801. Dr. Brink's present address is the Department of Anatomical Sciences, Health Sciences Center, State University of New York at Stony Brook, Stony Brook, New York 11704.

ABSTRACT It is generally thought that nexuses constitute low-resistance pathways between cell interiors in epithelial, neural, muscular, and even connective tissues. However, there are no reliable estimates of the specific resistance of a nexus. The reason for this is that in most cases the surfaces of nexuses between cells are geometrically complex and therefore it has been very hard to accurately estimate nexal areas. However, the septa of the median giant axon have a relatively simple shape. Moreover, in this preparation, it was possible to make a measuring current flow parallel to the axon axis so that from the voltage difference appearing between intracellular electrodes during current flow, the specific septal membrane resistance could be calculated. The average specific nexal resistance obtained was 5.9 Ω cm^2 if one assumes that 100% of the septum is nexus. The steady state I-V curve for the septum is linear ($\pm$10 mV). Placement of electrodes was validated by ionophoresing fluorescein into one of the cells. This allowed visualization of the septa even though the septa were found to be permeable to fluorescein and TEA. Exposure of the axon to hypertonic saline impedes the movement of fluorescein across the septa. By analogy with other tissues it is concluded that hypertonic solutions disrupt nexuses.

A mathematical model was derived which predicts the steady-state transmembrane potential vs. distance from a point source of intracellular current. When the specific nexal membrane resistance is 5.9 Ω cm^2, the prediction closely approximates the fall of transmembrane potential vs. distance in an ordinary infinite cable. This is commensurate with the electrophysiological behavior of this multicellular "axon."

INTRODUCTION

Electrical coupling between myocardial cells and smooth muscle cells has been shown to be sufficient for impulse propagation (Barr et al., 1965; Barr et al., 1968). Direct communication by diffusion between cell interiors has also been implicated as a mechanism for metabolic coupling (Subak-Sharpe et al., 1969). The only membrane junctional specialization common to vertebrate tissues where electrical or biochemical coupling has been shown is the nexus (McNutt and Weinstein, 1970, 1973). The intent of this study was to estimate the specific resistance of the nexal membrane and to estimate the permeability of the nexus to tetraethylammonium (TEA) and fluorescein. The effects of TEA, calcium, and hypertonicity were also investigated to help delineate the role of nexal membrane resistance in electronic spread.

Although organisms from the simplest metazoan up to mammals all possess nexus-like junctional membranes between specific cell types, preparations from most tissues contain large numbers of small cells. The junctions are not evenly distributed on the cells and the geometry of cells is often complex. To make an accurate calculation of nexal resistance, a system with large areas of nexus and no other junction present would be advantageous. The system would preferably be cable-like to allow one-dimensional analysis. A preparation that suits these needs is the median giant "axon" of the earthworm nerve cord.

In the earthworm the median giant axon is on the dorsal side of the ventral nerve cord. This axon actually is composed of many cells, cylindrical in shape, which are connected by specialized membrane structures. These specialized areas of relatively simple geometry were first seen by Stough (1926) who called them septa. Rushton (1945), Bullock (1945), Eccles et al. (1933), and later Kao and Grundfest (1957) showed that an action potential could travel along the axon in either direction. The ability to conduct in either direction, the small distances between the septa, and the fast conduction velocity made chemical synapses at the septa seem improbable. The septa are usually found where the segmental branches leave the nerve cord (Gunther, 1971) and are very often accompanied by a slight bulge. Stough (1926) showed that septa traverse the axon at an obtuse angle of about 150° going from the anterior to the posterior end. The area of the septum would then be approximately double the cross-sectional area of the axon. Closer examination of the septa by Dewey and Barr (1964) by electron microscopy revealed that a large fraction of the septa was nexus and that no other junctional type was present (see also Hamma, 1959; Coggeshall, 1965).

MATERIALS AND METHODS

Theory

A technique developed by Weidmann (1970) was employed to analyze the septa and axoplasmic resistances. The length of the nerve cord used was many times the space constant of the median giant axon (Goldman, 1964; Dierolf and Brink, 1973). The cord was surrounded by oil, with a thin film of saline left between the cord and the oil bath. Current pulses were applied via two agar-saline filled electrodes placed at the ends of the cord. It is shown that the current flow in this system can be described by the behavior of a one-dimensional cable (see Appendices A and B). As follows from cable theory, for preparations that are long relative to the length constant, there exists a region where the inside and outside currents run parallel with little or no transmembrane current. In this region there is no IR drop across the membrane, i.e. the potential difference between inside and outside due to current flow is zero.

In such a case, the determination of the current flowing longitudinally inside and the measurement of the voltage variation inside the axon with distance during a pulse, will allow the calculation of septa and axoplasmic resistance. This can be done easily because the total current is known and in the middle zone the intracellular and extracellular components distribute inversely to the respective resistivities.

Definition of Symbols

Because of the symmetry of the system we shall use the middle of the extracellular fluid layer as the reference point.

$V_0(x)$ = the electrical potential difference between any extracellular point and the

reference point; $V_i(x)$ = the electrical potential difference between any intracellular point and the reference point minus the resting potential; $V_m(x)$ = the transmembrane potential difference = $V_i(x) - V_0(x)$; $V_m(x) = I_m r_m$; $V_0^{AP}(x) = V_0(x)$ during a propagating action potential; $V_i^{AP}(x) = V_i(x)$ during a propagating action potential; $V_0^{pulse}(x)$ = steady state of $V_0(x)$ during a long constant current pulse; $V_i^{pulse}(x)$ = steady state value of $V_i(x)$ during a long constant current pulse; $I_0(x)$ = current in the extracellular space; $I_i(x)$ = current in the intracellular space; $I_m(x)$ = transmembrane current per unit length; $I_0^{AP}(x) = I_0(x)$ during a propagating action potential; $I_i^{AP}(x) = I_i(x)$ during a propagating action potential; $I_0^{pulse}(x) = I_0(x)$ during a pulse; $I_i^{pulse}(x) = I_i(x)$ during a pulse; r_m = resistance of membrane per unit length; r_0 = resistance of extracellular space per unit length; r_i = resistance of intracellular space per unit length; $r_i^{\Delta x}$ = resistance in intracellular space between two points Δx apart; $r_{axo}^{\Delta x}$ = resistance in intracellular space between two points Δx apart and with no intervening septum; r_s = resistance of the nexus(es) at a septum; θ = conduction velocity; R_{eff} = resistance between an inside point and an outside point away from which an axon extends indefinitely (see Appendix B). From Ohm's Law, in general

$$(dV_0(x)/dx)/r_0 = I_0(x), \tag{1}$$

$$(dV_i(x)/dx)/r_i = I_i(x). \tag{2}$$

For the case of an action potential at any point $I_0^{AP}(x_1) = I_i^{AP}(x_1)$ and for a wave propagating at a constant velocity (Katz, 1966):

$$dV_0^{AP}(x)/dx = 1/\theta dV_0^{(AP)}(x)/dt, \tag{3}$$

$$dV_i^{AP}(x)/dx = 1/\theta dV_i^{(AP)}(x)/dt. \tag{4}$$

Equating the currents in (1) and (2) and substituting for the spatial derivative from (3) and (4) results after rearrangement in:

$$\frac{dV_0^{AP}(x)/dt}{dV_i^{AP}(x)/dt} = \frac{r_0}{r_i}. \tag{5}$$

Now that we can calculate the resistance ratio, the current ratio during an applied pulse may be found to calculate the internal current. As a result of an applied pulse (I^{pulse}), current flow in the central region between electrodes separated by a large distance can be described as follows:

$$I_i^{pulse}(x) + I_0^{pulse}(x) = I_{pulse}. \tag{6}$$

Because there is no transmembrane current in the middle zone, for small x

$$V_m(x) = 0, \tag{7}$$

$$dV_i^{pulse}(x)/dx = dV_0^{pulse}(x)/dx, \tag{8}$$

from (1), (2) and (5)

$$\frac{\dfrac{dV_0^{pulse}(x)}{dx} \Big/ I_0^{pulse}(x)}{\dfrac{dV_i^{pulse}(x)}{dx} \Big/ I_i^{pulse}(x)} = \frac{r_0}{r_i}, \tag{9}$$

from (5) and rearrangement

$$\frac{dV_i^{AP}(x)/dt}{dV_0^{AP}(x)/dt} = \frac{I_0^{pulse}(x)}{I_i^{pulse}(x)}, \tag{10}$$

which reflects the dependence on the internal to external resistance ratio of both

observed AP ratio and the pulse current ratio. Substituting (6) into (10) and rearranging

$$I_i(x) = I_{pulse}/[1 + (dV_i^{AP}(x)/dt)(dV_0^{AP}(x)/dt)^{-1}]. \quad (11)$$

Substituting for the derivatives, the relevant approximations of finite differences to correspond to the actual measurements, we have from Ohm's Law in the middle zone

$$r_i^{\Delta x} = [\Delta V_i^{pulse}/I^{pulse}][1 + (\Delta V_i^{AP}(x)/\Delta t)(\Delta V_0^{AP}(x)/\Delta t)^{-1}], \quad (12)$$

if Δx is taken to include only one septum,

$$r_i^{\Delta x} = r_{axo} + r_s^{\Delta x}. \quad (13)$$

Equation (12) is essentially a statement of Ohm's law for internal current using variables which can be measured. Measurement of $\Delta V_i^{pulse}/\Delta x$ in an area away from a septum allows the calculation of $r_{axo}^{\Delta x}$ alone. The same measurement with a septum allows the calculation of r_s. Maximum rates of rise of the intracellular and extracellular action potentials were used for calculation of $\Delta V_i^{AP}/\Delta t$ and $\Delta V_0^{AP}/\Delta t$.

In order properly to analyze the septal resistances the assumption that a region exists where little current flows across the plasma membrane (i.e. where dV/dx equals a constant) had to be verified. Fig. 1 shows the steady-state voltage in the extracellular space and intracellular space as a function of distance in response to an applied current pulse recorded between a reference electrode, centered between the stimulating electrodes, and the recording electrode. The circles are the voltages recorded in the extracellular space, and the x's are the voltages recorded intracellularly. The measurements of septal and axoplasmic resistances were made in the region wherein the steady-state voltage outside the axon is the same as the steady-state voltage inside the axon.

Pyrex microelectrodes used for voltage measurements had resistances ranging from 10 to 20 MΩ when filled with 3 M KCl. Microelectrodes used for ionophoresis of fluorescein were filled with 0.1 M K citrate and then allowed to stand in a fluorescein solution. The fluorescein solution was made by adding to 80 ml of 1 M KOH 10 g of fluorescein and 3 g of K citrate, making the solution 0.38 M fluorecein and 0.1 M K citrate. Slow titration with H_3PO_4 brought the pH to 7.6 and kept the fluorescein in solution. Microelectrodes used for ionophoresis or hydraulic injection of 2.0 M TEA and 2.5 M calcium chloride were back filled.

For monitoring the fluorescence of fluorescein, a Brinkmann tungsten source was used with Brinkmann k530 barrier filter as well as an excitor blue FITC filter type 910031B (Brinkmann Instruments, Inc., Westbury, N. Y.). All densitometer measurements were made on a Weston photographic analyzer, model no. 877 (Weston, Inc., Newark, N.J.).

The hydraulic injections of TEA, calcium chloride, and fluorescein solutions followed the method of Grundfest et al., 1954.

Earthworms from Mogul-Ed (Oshkosh, Wis.) were identified as *Lumbricus terrestris* L. by the criterion of J. Stephenson (1930). They were maintained in a box 28 inches by 22 inches by 6 inches deep filled with a mixture of six parts soil, three parts mulch or leaves, and one part coffee grounds at 10°C for up to 2 wk. Earthworm saline (Prosser and Brown, 1950) was buffered by addition of 0.3 g/liter of trihydroxymethylamine methane (Tris). The pH was adjusted to 7.4 by addition of hydrochloric acid. Hypertonic saline was made by the addition of solid sucrose to isotonic saline (osmolarity = 780 mosmol, isotonic saline = 260 mosmol).

Earthworms were anesthetized in a 2% solution of MS 222 (tricaine methanesulfanate) for 2 or 3 min and the worms' nerve cords were dissected (Kao and Grundfest, 1957). The saline solutions used in the experiments all contained 27 μM carbachol to stop spontaneous contractions. No charge in membrane resistance, axoplasmic resistance, or the space constant could be detected in the presence of carbachol.

Although the length of the unattached nerve cord in saline was approximately 1.5 cm, after the cord had been pinned, it was stretched to 2.5 cm which was about its in vivo length. A septum was usually found near branches in the nerve cord and often a slight bulge in the giant axon could be seen in that region. Only septa found in the region where dV/dx was linear were used for measurement. Two microelectrodes were inserted 200–500 μm apart on both sides of a septum. The two extracellular recording electrodes were placed on the nerve cord about 4–7 mm apart. Mineral oil was added to the preparation, and the saline was removed by vacuum until a thin film of saline remained around the nerve cord. A stimulus was applied and the biphasic extracellular action potentials and

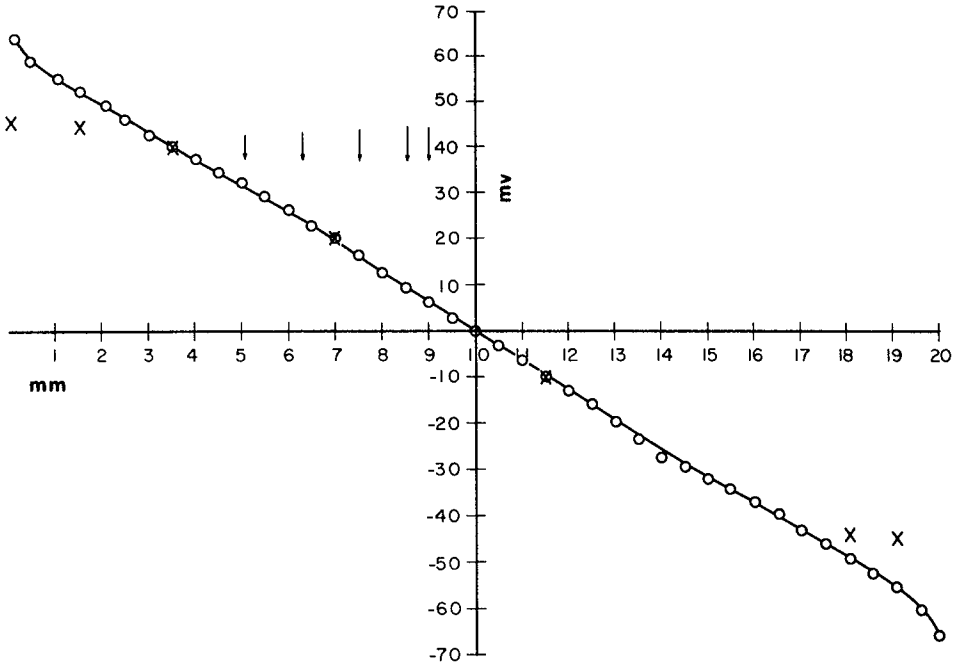

FIGURE 1. Steady-state voltage recorded as a function of distance when a current pulse was applied. Voltage was recorded between a reference electrode, centered between the stimulating electrodes, and a recording electrode. Circles represent the voltages recorded in the extracellular space; x = the voltages recorded in the intracellular space. Arrows indicate position of septa.

intracellular action potentials were recorded. The dV/dt was taken from both intracellular and extracellular action potentials and their ratio gave the ratio of parallel longitudinal resistances.

The change in the voltages between the two microelectrodes on either side of a septum in response to current pulses of various amplitudes was recorded. One microelectrode was removed and placed outside next to the other microelectrode still inside the axon, and the transmembrane voltage was recorded in response to the same current intensities. The transmembrane voltage change was never greater than a fraction of a millivolt in the region where dV/dx was linear when a current pulse was applied. If one assumes a uniform transmembrane potential in a cell 1 mm long and 50 μm wide and a plasma membrane resistivity of 10^4 Ω cm^2 (Goldman, 1964; Dierolf and Brink, 1973), a measured transmembrane voltage of 0.3 mV (largest value observed experimentally) indicates some

9.4×10^{-11} A flowing across the plasma membrane. The longitudinal current flow of 20 nA is therefore three orders of magnitude greater than that crossing the plasma membrane.

A microelectrode filled with fluorescein solution was always inserted into the cell where the septum was thought to be after axoplasmic measurements were made. The dye was ionophoresed into the cell with hyperpolarizing pulses of 20–30 nA and 20–30 ms in duration every 100 ms for 15–30 min. Since permeability of the septum to fluorescein is low, the septum appears clearly as a temporary barrier to the dye.

Conduction velocity measurements were made in a chamber which had four neighboring compartments in a row with small channels connecting adjacent compartments. Three compartments had diameters of 0.5 cm while one had a diameter of 1.5 cm (Fig. 2). Solutions were introduced on the floor of the large central chamber. A drain tube was placed at a level higher than the input line. In the median giant axon, the conduction

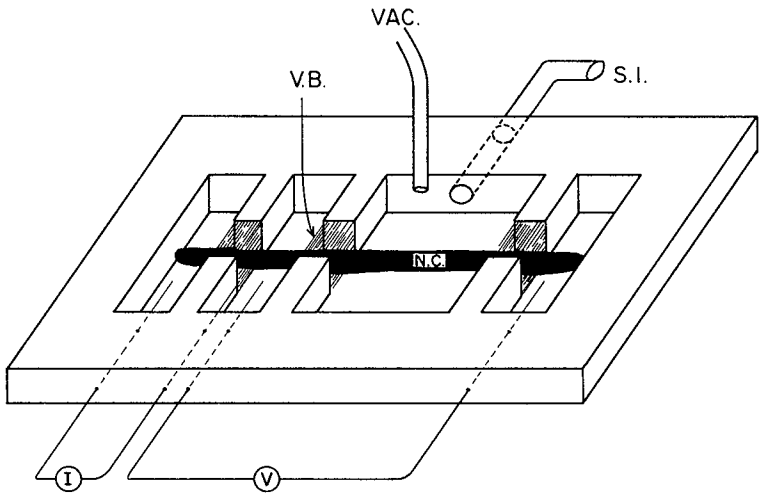

FIGURE 2. Nerve chamber used for measurement of conduction velocity in the presence of various saline solutions. *VAC*, vacuum; *VB*, Vaseline bridge; *SI*, solution input; V, the voltage recording apparatus; I, stimulus source.

velocity is slow enough to allow the action potential to be recorded across both Vaseline seals quite distinctly on a single oscilloscope sweep.

RESULTS

Septal Resistance

Fig. 3 illustrates the current voltage relationship of the septum in the giant axon. Varying intensities of steady-state current pulses were applied and the voltage drop across the septum was plotted as a function of the longitudinal current flow in the axon. In 12 experiments done in normal saline the current voltage curve was computed for the septa. In all cases the graphs were linear. The correlation coefficient varied from 0.97 to 0.99.

Table I summarizes the results of 18 experiments in normal saline in which septal resistance was calculated. The average value of the septal membrane resistance (r_s) was 38 kΩ. The septal membrane resistance was calculated by assuming that a septum runs across the axon at an angle of about 150° (Stough,

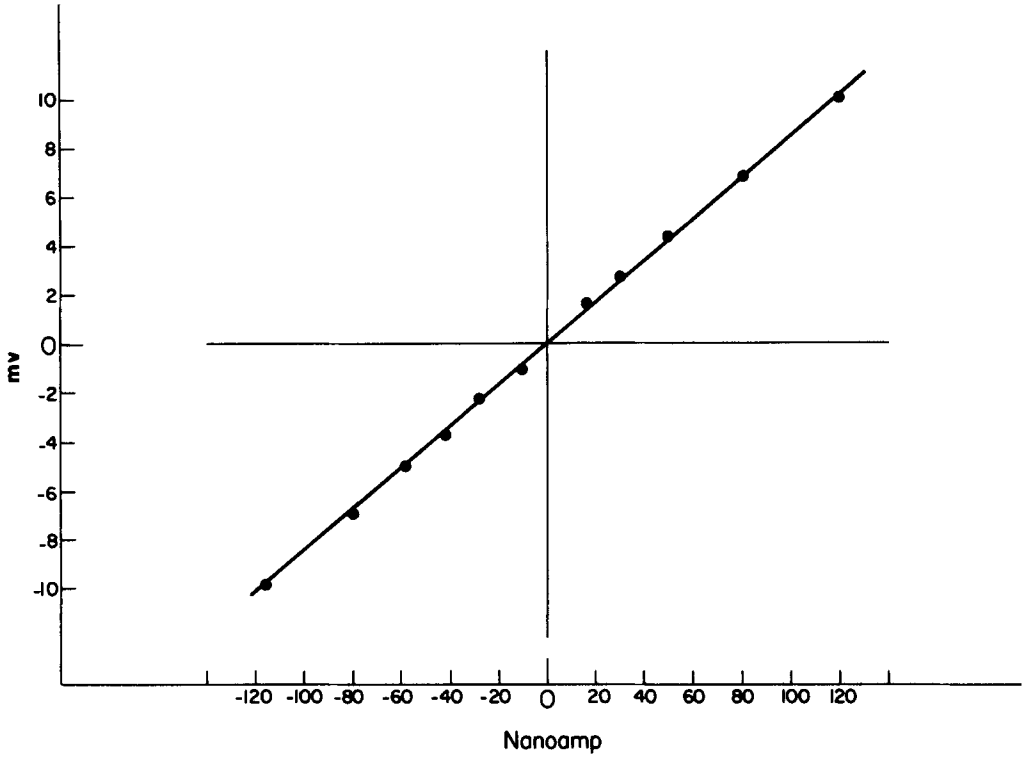

FIGURE 3. I-V curve for a septum in a giant axon in the nerve cord of the earthworm. Long-duration current pulses were applied. The septal voltage and longitudinal current in the axon were measured and plotted.

TABLE I

SEPTAL MEMBRANE RESISTANCE

	dV_i/dt	dV_o/dt	Cell length	r_a	R_a	r_s	R_s
	mV/ms	*mV/ms*	*mm*	*kΩ*	*Ω cm*	*kΩ*	*Ω cm²*
Range	330–665	6.2–33.0	0.7–2.00	140–950	149–420	19–85	1.5–12.5
Mean	457	18.7	1.21	365	229	38	5.9
SEM	±24	±1.8	±0.08	±3.2	±12	±0.41	±0.71

dV_i/dt = the slope measured from the fast rate of rise of the intracellularly recorded action potential.
dV_o/dt = the slope measured from the fast rate of rise of the extracellularly recorded action potential.
Cell length was measured as the distance from septum to septum from the cell in which axoplasmic and septal voltage measurements were made. The positions of the septa were revealed by dye injection.
r_a = the total cytoplasmic resistance in ohms of each cell where measurements were made.
R_a = the axoplasmic resistivity.
r_s = the resistance of a septum in ohms.
R_s = the septal membrane resistance in ohms cm².

1926). The average area of a septum was 1.5×10^{-4} cm². If the total surface area of the septal membrane were nexus, then the specific nexal membrane resistance would be 5.9 Ω cm². The cell length was measured from septum to septum as revealed by the dye injection.

The effect of TEA of septal resistance was measured and the data are given in Table II. TEA was found to diffuse well beyond the septum of the injected cells. TEA was ionophoresed into the axon by applying 15-nA depolarizing pulses, 20 ms long, every 70 ms for 2 h and 45 min. At the end of the injection, the effect of TEA on the action potential was taken as the change in the duration as measured at one-half the height of the action potential. The injection and recording points were within 500 μm of the septum which was later revealed by fluorescein injection. 250 μm away from the septum on the noninjected side, the duration of the action potential was increased by a factor of 3, while in the injected cell the duration was 3.5 times greater than the action potential duration before TEA application. The duration of the action potential was increased by a factor of 1.3 at a distance of 1.5 mm away from the septum, and at 5 mm away no increase in duration of the action potential could be observed. No difference in the septal resistance before and after TEA application was observed. The injected cell was

TABLE II

EFFECT OF TEA AND FLUORESCEIN ON SEPTAL RESISTANCE

dV_i/dt	dv_0/dt	Cell length	r_a	R_a	r_s	R_s
mV/ms	*mV/ms*	*mm*	*kΩ*	*Ω cm*	*kΩ*	*Ω cm²*
TEA injection control						
500	15	1.8	700	310	30	4.7
TEA ionophoresis (2 h 45 min)						
450	14	–	690	305	29	4.5
Fluorescein injection control						
475	20	0.9	230	210	43	6.7
Fluorescein ionophoresis (30 min)						
460	19	–	240	220	43	6.7

For definitions see legend to Table I.

slightly depolarized after injection. Recently, Weingart (1974) using the method of Weidmann (1966) showed that radioactive TEA diffuses easily down bundles of ungulate myocardium.

Septal and axoplasmic resistances were calculated before and after a 30-min period of ionophoresis of fluorescein into the cell and no change in R_s or R_a was observed, as shown in Table II. No change in resting potential was observed (−68 mV). There were no changes in the transmembrane voltages recorded in response to current pulses injected via microelectrodes between controls and TEA or fluorescein injections.

Calcium Injection

In four experiments after the measurement of septal and axoplasmic voltages, a microelectrode filled with 2.5 M calcium chloride was inserted into the cell where the axoplasmic measurements were made. 20-nA depolarizing pulses 20 ms long were applied every 100 ms. Within minutes the injected cell was depolarized and an action potential could not be elicited from that cell. The plasma membrane

resistance decreased continuously as calcium was injected. For these reasons the septal resistance could not be estimated in these experiments. Because calcium has been shown by Hodgkin and Keynes (1957) to bind in the axoplasm of squid axon, we could not know intracellular calcium concentration at the septum of the injected cell even if an effect on septal resistance could be observed. Cells adjacent to the calcium-injected cells showed some depolarization within a few minutes after termination of calcium ionophoresis, thus calcium may be able to pass through the nexal membranes.

Anisotonic Solutions

In some experiments, after the septal and axoplasmic resistance calculations were made, the normal saline was exchanged for hypertonic saline (3×). The

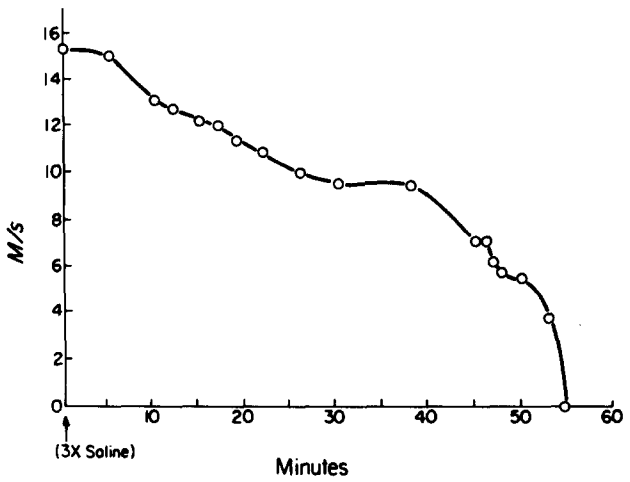

FIGURE 4. Conduction velocity as a function of time in hypertonic saline (3×). The arrow indicates when the hypertonic saline was added. Conduction velocity was measured via the Vaseline bridge method as described in Materials and Methods.

exchange of solutions under oil was difficult and in some cases caused spontaneous contractions of the nerve cord. Application of hypertonic solutions caused depolarization of the axon membrane and conduction failure. The resting potential along the axon also varied from −20 mV to −45 mV in hypertonic solution after a 60-min exposure. Because conduction velocity failed and membrane potentials were decreased, it was impossible to measure septal and axoplasmic resistances. Fig. 4 shows the effect of hypertonic saline (3×) on conduction velocity with time. Conduction is decreased and finally fails. Membrane depolarization could be causing this effect, but disruption of nexal membranes is also a possibility.

Fig. 5 shows the external voltage as a function of distance between a reference electrode, centered between the stimulation electrodes, and a recording electrode when a steady-state current pulse was applied while the preparation was in hypertonic saline. The transmembrane voltage equals that of the extracellular

space even at the extreme ends of the preparation near the stimulating electrodes. This is contrasted to the normal situation in isotonic saline where there is a difference between V_i and V_0 in close proximity to stimulating electrodes due to transmembrane current flow (Fig. 1). Intermediate situations, where an action potential was slowed, were so difficult to obtain that the effects on resistance of hypertonic saline were not analyzable.

Since fluorescein passes the septum with a time constant of approximately 1 h, it can be used to detect changes in septal permeability. Fig. 6 is a graph of the

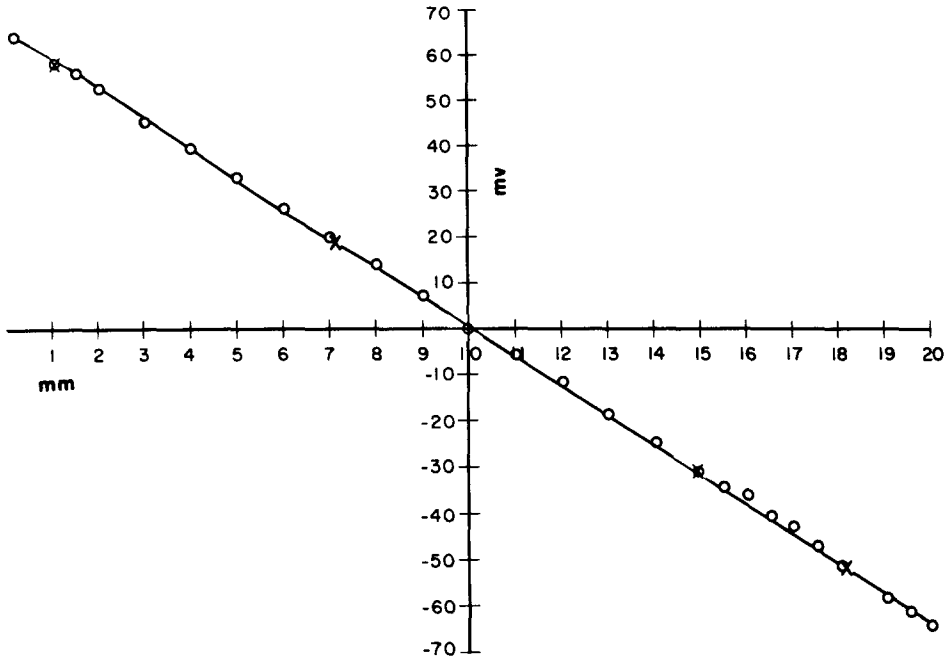

FIGURE 5. The steady-state voltage recorded as a function of distance when a current pulse was applied after the axon had been standing in hypertonic saline (3×) for 30 min. Voltage was recorded between a reference electrode centered between the stimulating electrodes and a recording electrode. Circles are the voltages recorded in the extracellular space; x = voltages recorded in the intracellular space.

intensity of fluorescence of ionophoresed fluorescein in a cell vs. distance along a giant axon in normal solutions. Photographs of the injected cell were made at various time intervals. With each negative, background measurements were made and subtracted from the measured intensities in the axon. The intensity measured at the time zero in the injected cell of the axon was taken as 100% intensity. During the entire experiment, that is dye injection and photographing, the nerve cord was surrounded by hypertonic saline (3×). Comparison of Figs. 6 and 7 shows that fluorescein trans-septal movement is blocked by hypertonic saline. One explanation for the block of fluorescein movement is that the nexuses which in part make up the septal membrane are disrupted by hyper-

tonic solutions. At very long times (~3 h) some fluorescein can be seen apparently traversing the septum, but this may be explained by movement of dye in the extracellular space or by the possibility that not all nexal area is disrupted.

A Model for the Earthworm Median Giant Axon

We have compared the prediction of a simple model, which incorporates our results, with the exponential spread of current along a cable. This comparison demonstrates the effect of the existence of the extra, nexal resistances at the

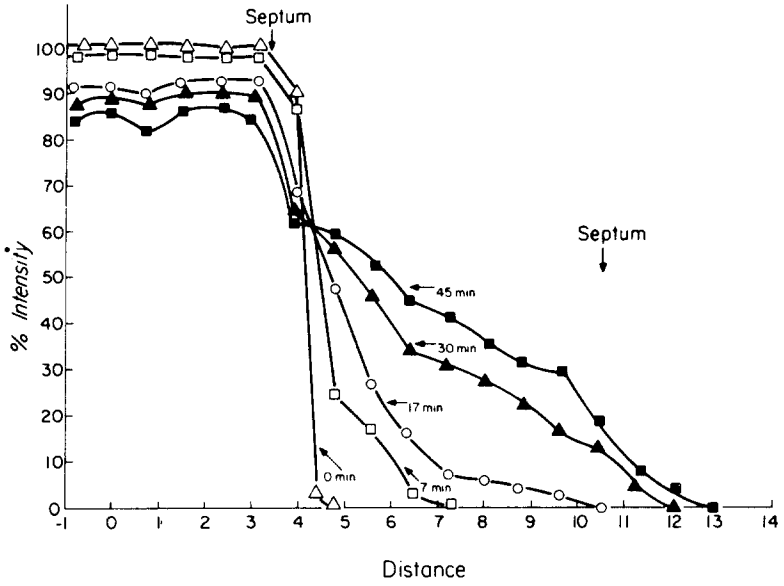

FIGURE 6. Fluorescence of fluorescein in an axon in isotonic saline measured as a function of distance at varying time intervals after termination of the injection period. The time intervals were time zero (triangles), 7 min (squares), 17 min (circles), 30 min (filled triangles), and 45 min (filled squares). The vertical axis represents per cent original intensity. The arrows indicate the positions of the septa along the axon (see text). Distance was measured from the injection electrode. Horizontal axis units are in 100-μm divisions.

septa in the internal pathway. Since the earthworm median giant axon is made up of many cylindrical cells attached to one another end to end by nexuses at the septa, it can be considered as many finite cables in series connected to each other by finite resistances (see Appendix B). The general equation describing the first segment is:

$$\lambda^2 \frac{d^2V}{dx^2} = V, \tag{14}$$

where we take V as V_m as described above. If current is passed between an internal point and another immediately outside an EMGA, the internal current I_i aproaches the transnexal current I_n at the end of an axonal segment. Therefore,

$$d[V_m(L)]/dx = I_n(r_i + r_0), \quad (a)$$

and

$$V_m(L) = I_n(R_{eff} + r_s), \quad (b)$$

as x approaches L from $x < L$ and $V_m(L) = I_n R_{eff}$ as x approaches L $x > L$; L being the segment length. Application of these boundary conditions (see Appendix B) yields the following solution for the steady-state transmembrane potential for distances up to the first septum

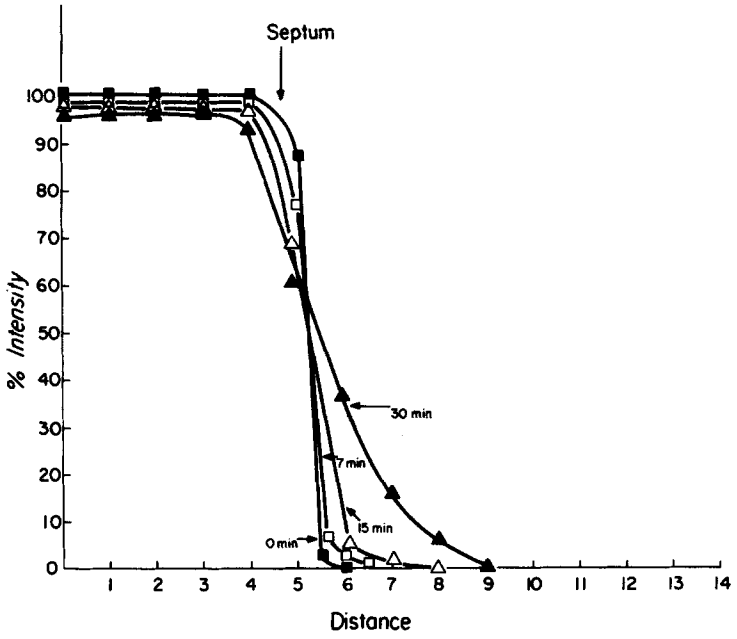

FIGURE 7. An experiment and analysis identical to those in Fig. 6 were performed but the axon was in hypertonic saline throughout the ionophoretic and photographic periods. Photographs were taken at time zero (filled squares), 7 min (squares), 15 min (triangles), and 30 min (filled triangles) after termination of dye injection. Horizontal axis units are in 100-μm divisions.

$$V_m(x) = V_m(o)\frac{(R_{eff} + r_s)\cosh[(L - x)/\lambda)[+ \lambda(r_i + r_o)\sinh[(L - x)/\lambda]}{(R_{eff} + r_s)\cosh(L/\lambda) + \lambda(r_i + r_o)\sinh(L/\lambda)}, \quad (15)$$

and the trans-septal current

$$I_n = V_m(o)/[\lambda(r_i + r_o)\sinh(L/\lambda) + (R_{eff} + r_s)\cosh(L/\lambda)]. \quad (16)$$

For the next segment the transmembrane voltage was calculated by using Eq. (15) but setting $V_m(o)$ for that segment, equal to $I_n R_{eff}$ where I_n was calculated from Eq. (16) for the first segment. The process can be repeated indefinitely. Fig. 8 shows the graphic solutions of the equation where R_s = 30,000 Ω and r_s = 500,000 Ω. The solution for an infinite cable is also included in the calculations

made for Fig. 8: the space constant equalled 3.55 mm, the septa occurred every 1 mm (L), and V_0 equalled 30 mV. The similarity of the 30 kΩ curve to the exponential would seem to preclude any experimental distinction between them. This would conform to our results.

DISCUSSION

Our range of septal specific resistance was 1.5–12.5 Ω cm². If the nexus covered 100% of the septum, then the values are equivalent to nexal specific resistance. If

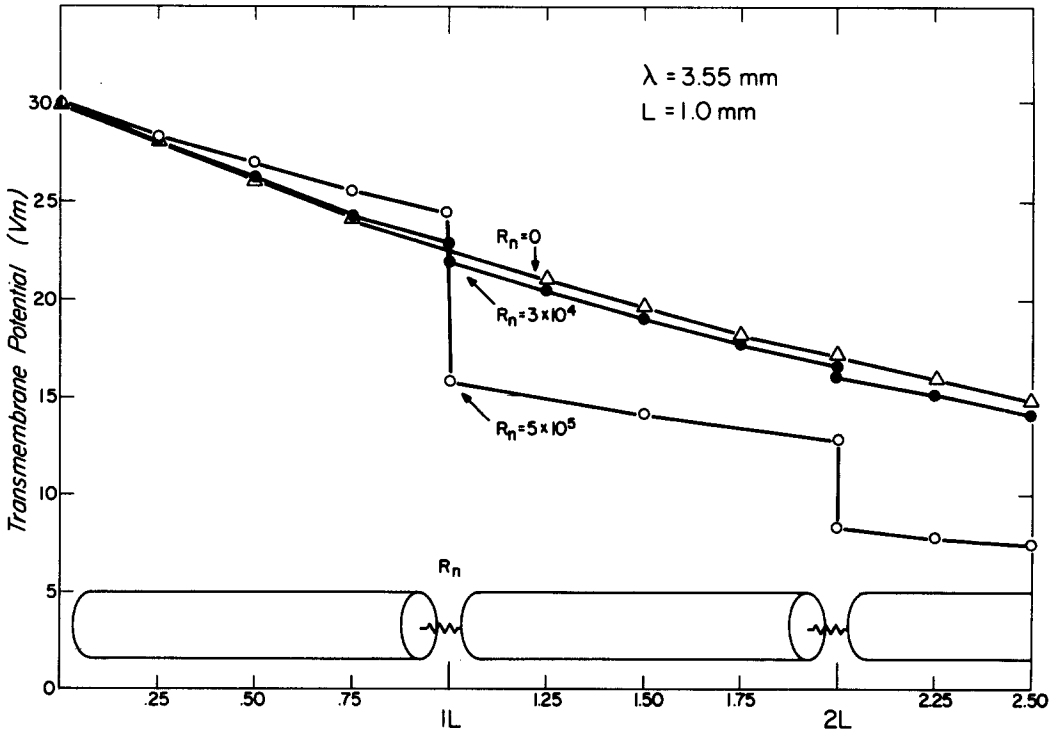

FIGURE 8. Graphic solutions of transmembrane potential vs. distance when a constant current pulse is applied to a model septate axon.

the average area of nexus was only 10% the total surface of a septum, the nexal resistance would range from 0.15 to 1.25 Ω cm². If the nexal membrane area were larger due to folding, the nexal resistance would be higher. This range of values for nexal membrane resistance is within the range of nexal membrane resistances previously reported (Kriebel, 1967; Weidmann, 1966). The conductance of nexal membranes is three orders of magnitude higher than the plasma membrane, and it can be concluded that the nexus is a low-resistance pathway between cells in the giant axon.

It has been suggested that a pore 1.0–2.0 nm in diameter is located in the center of the particles which make up a nexus (McNutt and Weinstein, 1970). If one assumes that the conductance of the pore is the same as an equivalent amount of

axoplasm, calculations can be made to estimate the lower limit on the number of pores needed to give specific septal resistance of 5.9 Ω cm^2. If $r_p = r_a L/A$ where r_a equals the resistivity of cytoplasm (200 Ω-cm), and r_p equals resistance of a pore in ohms, and A equals cross-sectional area of the pore, and L equals length of the pore. If one assumes that the pore is 18 nm in length and has a cross-sectional area of 3.14×10^{-14} cm^2, the hypothetical resistance of a pore is then $r_p = 1.15 \times 10^{10}$ Ω.

Given that the particles are arranged in an hexagonal array where the center to center distance is 9 nm, the number of pores per 1 cm^2 is 1.4×10^{12}, and the specific nexal resistance would be 8×10^{-3} Ω cm^2. This value is three orders of magnitude less than the observed value of 5.9 Ω cm^2. On the basis of his morphological data on rat myocardium, Matter (1973) has calculated a value of 5.1×10^{-2} Ω cm^2 which contrasts similarly with available physiological data. Obviously, no account was made in the previous calculation for the effect of frictional forces or fixed charges that may or may not exist in the pore. If approximately 70% of the septal membrane area were nexus, the total area of nexus would be 1.2×10^{-4} cm^2 and there would be 1.7×10^8 pores. To achieve a specific nexal membrane resistance (R_s) of 5.9 Ω cm^2 or septal resistance (r_s) or 30,000 Ω, each pore would have to have a resistance of $r_p = 5.7 \times 10^{12}$ Ω. Consequently, the axoplasmic resistance (R_a) in such a pore would have to be 100,000 Ω cm or 500 times the bulk axoplasmic resistance. A pore axoplasmic resistance of 100,000 Ω cm is conceivable only if there are frictional forces or fixed charges at work retarding the movement of ions as they pass through a pore. Another explanation for increased axoplasmic resistance in the pore might be smaller pore sizes. But to attain a pore resistance of 5.7×10^{12} Ω when R_a equals 200 Ω cm, the pore diameter would have to be 0.09 nm. This low value would not permit the diffusion even of potassium ions much less fluorescein. Clearly the diffusion of larger molecules such as Kolodny's (1971) macromolecular RNA, microperoxidase (Reese et al., 1971), and Procion yellow (Imanaga, 1974) would be impossible.

Since potassium is the principal ion on either side of a nexus and cytoplasmic calcium is very low, the bearing of the TEA experiments on the possibility that the nexus is traversed by potassium channels is significant. TEA was iontophoresed because of its well-known inhibition of the activation of potassium channels, since by analogy with the linear I-V curve for squid plasma membrane (Rojas and Ehrenstein, 1965) one might presume the high nexus conductance is due to activated potassium channels. Therefore, TEA might decrease the nexal conductance. This was not realized. Moreover, TEA crossed septal membranes much more readily than it does plasma membrane.

The results of the hypertonic experiments were consistent with results that show nexal disruption in hypertonic media but could be also explained as a decrease in plasma membrane resistance. However, the fact that the flow of fluorescein is essentially stoppped at a septum in the axon in hypertonic saline probably means that nexal membranes have separated interfering with the longitudinal path for the dye. Reduction in plasma membrane resistance in hypertonic saline might allow greater loss of dye through the plasma membrane, thereby decreasing the amount of dye moving along the long axis. However, if

this were the case, then the fluorescent intensity of the injected cell in hypertonic saline would be expected to fall more rapidly than that of normal saline when, in fact, just the opposite occurs.

The value of axoplasmic resistance (R_a) is in good agreement with previous estimates of axoplasmic resistance (Goldman, 1964; Dierolf and Brink, 1973). The cell length measurement was made to allow computation of the total cytoplasmic resistance (r_a) of a cell so that comparison of the cytoplasmic resistance with the septal resistance (r_s) could be made. Unfortunately, there is no internal standard similar to the sarcomere to determine the proper length of stretch. To combat this problem from preparation to preparation, efforts were made to dissect nerve cords of similar length. The average cell length should be considered a very rough estimate of the average distance between septa.

In summary, the nexal membrane complex has been shown to have a low resistance relative to the plasma membrane. It is a nonrectifying structure over a voltage range of ±10 mV. Since anionic fluorescein and cationic TEA will cross the septum, the role of the nexus in the formation of metabolic coupling needs further clarification by use of techniques such as autoradiography. However, in the earthworm as well as in other examples from widely separated species, the nexal pores seem to be large enough to allow intermixing of metabolically important molecules (Gilula, 1974). Thus it is as important to cellular communication as the plasma membrane is to the maintenance of the internal milieu of cells. Although the nexus may have been one of the first evolutionary steps going from unicellular to multicellular organisms, there is evidence that nexuses from different tissues or organisms may vary considerably in fine structure (Gilula, 1974).

APPENDIX A

To analyze our experimental situation in more general terms, consider a segment of a nonmyelinated axon sealed at each end and submerged in paraffin oil so that the outside of the axon is covered by a thin layer of aqueous solution. In addition, small punctate electrodes are touched to the external layer at the very ends of the axon. In order to derive a relatively simple mathematical description of the electrical behavior of this system we will stipulate as is commonly done (Hodgkin and Rushton, 1946; Cole, 1968) that:

(*a*) all resistances are constant;
(*b*) the external layer and the axon are thin enough and the membrane resistance is high enough so that the internal and external electrical potentials are functions of distance along the axon only;
(*c*) a steady state is present; i.e., capacitive transients can be ignored;
(*d*) $\lambda^2 = r_m/(r_o + r_i)$;
(*e*) I_o (x) and I_i (x) are positive when going from right to left and I_m (x) is positive when going outward;
(*f*) other symbol are as given earlier;
(*g*) the electrodes are point sources and sinks of current at exactly the ends of a segment of the axon.

The lumped parameter representation of this finite one-dimensional cable is shown in Fig. 1 A. The equation for the continuous case is

$$\lambda^2 d^2 [V_m (x)]/dx^2 - V_m (x) = 0, \quad (1)$$

which has the general solution

$$V_m(x) = C \sinh(x/\lambda) + C_1 \cosh(x/\lambda), \tag{2}$$

because of symmetry $V_m(o) = 0$, therefore $C_1 = 0$, and thus

$$V_m(x) = C \sinh(x/\lambda), \tag{3}$$

since $I_i(-L) = 0$.

$$\begin{aligned} I_i(x) &= \int_{-L}^{x} I_m dx = \int_{-L}^{x} (C/r_m)\sinh(x/\lambda)dx \\ &= (C\lambda/r_m)[\cosh(x/\lambda) - \cosh(L/\lambda)], \end{aligned} \tag{4}$$

further, $I_{pulse} = I_o(-L)$ and $dV_i(-L)/dx = 0$, therefore

$$\begin{aligned} dV_m(-L)/dx &= -dV_o(-L)/dx \\ (C/\lambda)\cosh(-L/\lambda) &= -r_o I_{pulse} \\ C &= -\lambda r_o I_{pulse} \operatorname{sech}(L/\lambda), \end{aligned} \tag{5}$$

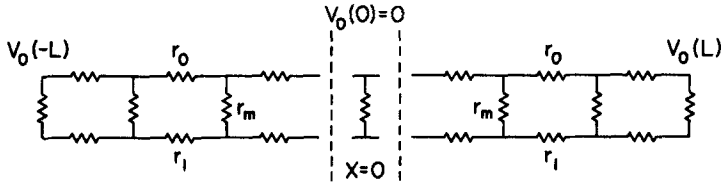

FIGURE 1 A. Equivalent circuit for an axon of length $2L$. Stimulating electrodes are placed at both ends as described in Materials and Methods. r_m, the membrane resistance; r_0, extracellular fluid resistance; r_i axoplasmic resistances.

therefore

$$V_m(x) = -\lambda r_o I_{pulse} \operatorname{sech}(L/\lambda)\sinh(x/\lambda). \tag{6}$$

The conditions under which the common assumption (Hodgkin and Rushton, 1946),

$$I_i(x) = I_{pulse}\, r_o/(r_o + r_i),$$

holds may be seen from noting that this is equivalent to setting $dV_i(x)/dx = dV_o(x)/dx$

$$[dV_o(x)/dx]/[dV_i(x)/dx] = [dV_i(x)/dx - dV_m(x)/dx]/[dV_i(x)/dx], \tag{7}$$

upon substitution and rearrangement

$$\begin{aligned} &[dV_o(x)]/[dV_i(x)/dx \\ &\quad = [r_i + r_o \cosh(x/\lambda)/\cosh(L/\lambda)]/[r_i - r_i \cosh(x/\lambda)/\cosh(L_J\lambda)], \end{aligned} \tag{8}$$

for the earthworm axon λ may be taken as less than 4 mm. If preparations 4 cm long are used, $\cosh(L/\lambda)/\simeq 75$ and the assumption will hold quite well for the middle centimeter or so. If the preparation is longer, the accuracy of the assumption increases very rapidly because of the dependence of $\cosh(L/\lambda)$. That the preparation behaves in the center region like two parallel resistances can be seen from considering the first of the two terms describing the effective resistance between the electrodes

$$R_{eff} = 2V_o(L)/I_{pulse} = 2[r_i \int_o^L I_i(x)\, dx - V_m(L)]/I_{pulse}, \tag{9}$$

$$R_{\text{eff}} = \frac{2r_i r_o \lambda}{r_i r_o} L + \frac{2\lambda r_o^2}{r_i r_o} \tanh (L/\lambda). \tag{10}$$

APPENDIX B

The influence of the nexal resistances at the septa of the earthworm median giant axon may be considered by seeing how they enter into the expression for changes of transmembrane voltage as a function of distance when a constant current is injected into an axon via a microelectrode. In a very long, nonseptate, nonmyelinated axon this of course would be described by the familiar

$$V_m (x) = V_m (o)\, e^{-x/\lambda}. \tag{1}$$

In order to examine the more complicated septate case we stipulate:

(*a*) the first six stipulations of Appendix A;

(*b*) the axon is made up of one-dimensional cable segments of length L which are connected directly in the external path and connected via a nexal resistance R_n in the internal path at the septa;

(*c*) current, I_{pulse}, is passed between internal and external point electrodes placed at one end of a segment away from which the axon extends indefinitely;

(*d*) the current across the first septum is I_n (Fig. 1 B).

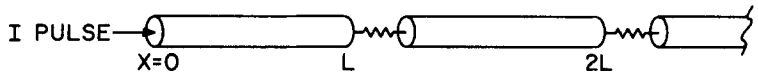

FIGURE 1 B. Schematic representation of segmental axon. L = the position of the septa. Each cell is connected to an adjacent cell by a septal resistance. I_{pulse} is the value of the total applied current.

For the first segment the situation is equivalent to a finite cable terminated by a finite resistance, $(r_s + R_{eff})$, where R_{eff} is equal to the effective resistance between the two point electrodes. A general solution for the region $x<L$ is

$$V_m (x) = C_1 \cosh (x/\lambda) + C_2 \sinh (x/\lambda). \tag{2}$$

From $dV_m (x)/dx = dV_i (x)/dx - dV_o (x)/dx$ and Ohm's law

$$\frac{dV_m (L)}{dx} = I_n (r_i + r_o), \tag{3}$$

and from Ohm's law

$$V_m (L) = I_n (r_s + R_{eff}), \tag{4}$$

combining to eliminate I_n

$$V_m (L) = -(r_s + R_{eff})/(r_i + r_o) \frac{dV_m (L)}{dx}, \tag{5}$$

from (2) at $x = L$

$$V_m (L) = C_1 \cosh (L/\lambda) + C_2 \sinh (L/\lambda), \tag{6}$$

$$\frac{dV_m(L)}{dx} = (C_1/\lambda) \sinh (L/\lambda) + (C_2/\lambda) \cosh (L/\lambda), \tag{7}$$

and from (2) at $x = 0$

$$V_m (o) = C_1, \tag{8}$$

substituting into (5)

$$V_m(o)\cosh(L/\lambda) + C_2\sinh(L/\lambda) = -\frac{(r_s + R_{eff})}{r_i + r_o}[(V_m(o)/\lambda)\sinh(L/\lambda) + (C_2/\lambda)\cosh L/\lambda], \tag{9}$$

rearranging

$$C_2 = -\frac{V_o\{\cosh L/\lambda + [(r_s + R_{eff})/\lambda(r_i + r_o)]\sinh L/\lambda\}}{\{[(r_s + R_{eff})/\lambda(r_i + r_o)]\cosh(L/\lambda)\} + \sinh(L/\lambda)}, \tag{10}$$

$$V_m(x) = V_m(o)\frac{(r_s + R_{eff})\cosh[(L - x)/\lambda] + \lambda(r_i + r_o)\sinh[(L - x)/\lambda]}{(r_s + R_{eff})\cosh(L/\lambda) + \lambda(r_i + r_o)\sinh(L/\lambda)}. \tag{11}$$

An expression for R_{eff} as a function of L, r_s, r_i, r_o, and r_m is still required in order to compute $V_m(x)$ using (11). By definition

$$R_{eff} = V_m(o)/I_{pulse}, \tag{12}$$

and also since the axon is indefinitely long

$$R_{eff} = [V_m(L) - I_n r_s]/I_n, \tag{13}$$

where, the current out of the first segment is:

$$I_n = I_{pulse} - \int_o^L I_m\,dx, \tag{14}$$

therefore,

$$I_n = I_{pulse} - \int_o^L \frac{V_m(x)}{r_m}\,dx,$$

setting

$$K = \frac{1}{r_m V_m(o)}\int_o^L V_m(x)\,dx = \frac{\lambda^2(r_i + r_o)[\cosh(L/\lambda) - 1] + \lambda(r_s + R_{eff})\sinh(L/\lambda)}{r_m[(r_s + R_{eff})\cosh(L/\lambda) + (r_i + r_o)\sinh(L/\lambda)]},$$

and

$$F = V_m(L)/V_m(o) = \frac{r_s + R_{eff}}{[(r_s + R_{eff})\cosh(L/\lambda) + \lambda(r_i + r_o)\sinh(L/\lambda)]},$$

upon substituting into (13)

$$R_{eff} = \frac{[V_m(o)F - (I_{pulse} - V_m(o)K)r_s]}{I_{pulse} - V_m(o)K}, \tag{15}$$

substituting from (12) for $V_m(o)$ and rearranging

$$R_{eff}K^2 + (r_xK + F - 1)R_{eff} - r_s = 0. \tag{16}$$

If this is multiplied out, a cubic equation of the form

$$AR_{eff}^3 + BR_{eff}^2 + CR_{eff} + D = 0, \tag{17}$$

results, where:

$$A = \lambda \sinh(L/\lambda);$$
$$B = 2\lambda r_s \sinh(L/\lambda);$$
$$C = \lambda r_s^2 \sinh(L/\lambda) - \lambda r_m (r_i + r_o)\sinh(L/\lambda) - r_s r_m \cosh(L/\lambda);$$
$$D = r_s r_m [r_s \cosh(L/\lambda) + \lambda(r_i + r_o)\sinh(L/\lambda)].$$

The only real positive root of this cubic equation may be easily computed. When $r_s = 3 \times 10^4\,\Omega$, $r_m = 3 \times 10^5\,\Omega\,\text{cm}^2$, $r_i = 3 \times 10^6\,\Omega/\text{cm}$, $r_o = 0$ and $L = 0.1$ cm, $R_{\text{eff}} = 1.03 \times 10^6\,\Omega$. This is only 1.08 times $\sqrt{r_m r_i}$, which is the equivalent for an equivalent nonseptate axon.

The authors would like to thank Drs. Erik Jakobsson and Maynard Dewey for their valuable discussions.

This work was supported in part by National Institutes of Health grant HE 14125.

Received for publication 24 March 1976.

REFERENCES

BARR, L., W. BERGER, and M. DEWEY. 1968. Electrical transmission at nexus between smooth muscle cells. *J. Gen. Physiol.* **51**:347–368.

BARR, L., M. DEWEY, and W. BERGER. 1965. Propagation of action potential and structure of the nexus in cardiac muscle. *J. Gen. Physiol.* **48**:797–823.

BULLOCK, T. H. 1945. Functional organization of the giant fiber system of *Lumbricus*. *J. Neurophysiol.* **8**:55–71.

COGGESHALL, R. 1965. A fine structure analysis of the ventral nerve cord of the associated sheath of *L. terrestris*. *J. Comp. Neurol.* **125**:393–407.

COLE, K. S. 1968. Membranes, Ions and Impulses. University of California Press. 64 et seq.

DEWEY, M., and L. BARR. 1964. A study of the structure and distribution of the nexus. *J. Cell Biol.* **23**:553–585.

DIEROLF, B., and P. BRINK. 1973. Effects of thermal acclimation on cable constants of the earthworm median giant axon. *Comp. Biochem. Physiol.* **44A**:401–406.

ECCLES, J., R. GRANIT, and J. Z. YOUNG. 1933. Impulses in the giant nerve fibres of earthworm. *J. Physiol. (Lond.)*. **77**:23P–25P.

GILULA, N. 1974. Junctions between cells. *In* Cell Communication. R. P. Cox, editor. John Wiley & Sons, New York. 1–29.

GOLDMAN, L. 1964. The effects of stretch on cable and spike parameters of single nerve fibers; some implications for the theory of impulse propagation. *J. Physiol. (Lond.)*. **175**:425–444.

GRUNDFEST, H., C. Y. KAO, and M. ALTAMIRANO. 1954. Bioelectric effects of ions microinjected into the giant axon of leligo. *J. Gen. Physiol.* **38**:(2, Pt. 2):245–282.

GUNTHER, J. 1971. Der cytologische Aufbau der dorsalen Riensenfaser von *Lumbricus terrestris*. *Z. Wiss. Zool.* **183**:51–70.

HAMMA, K. 1959. Some observations on the fine structure of the giant nerve fibers of the earthworm *Eisenia foetida*. *J. Biophys. Biochem. Cytol.* **6**:61–66.

HODGKIN, A. L. and W. A. H. RUSHTON. 1946. The electrical constants of a crustacean nerve fibre. Proc. R. Soc. Lond. *Ser. B Biol. Sci.* **133**:444–479.

HODGKIN, A. L., and R. D. KEYNES. 1957. Movements of labelled calcium in squid giant axons. *J. Physiol. (Lond.)*. **138**:253–281.

IMANAGA, I. 1974. Cell to cell diffusion of Procion yellow in sheep and calf Purkinje fiber. *J. Membr. Biol.* **16**:381–388.

KAO, C. Y., and H. GRUNDFEST. 1957. Postsynaptic electrogenesis in septate giant axons. I. Earthworm median giant axon. *J. Neurophysiol.* **20**:553–573.

KATZ, B. 1966. Nerve, Muscle and Synapse. McGraw-Hill Book Co., New York.

KOLODNY, G. M. 1971. Evidence for transfer of macromolecular RNA between mammalian cells in culture. *Exp. Cell Res.* **65**:313–324.

KRIEBEL, M. E. 1967. Electrical characteristics of tunicate heart cell membranes and nexuses. *J. Gen. Physiol.* **52**:46–59.

MCNUTT, N. S., and R. WEINSTEIN. 1970. The ultrastructure of the nexus. *J. Cell Biol.* **47**:666–688.

MCNUTT, N. S., and R. S. WEINSTEIN. 1973. Membrane ultrastructure and mammalian intercellular junctions. *Prog. Biophys. Mol. Biol.* **26**:45–97.

MATTER, A. 1973. A morphometric study on the nexus of rat cardiac muscle. *J. Cell Biol.* **56**:690–696.

PROSSER, C. L., and F. A. BROWN. 1950. Comparative Animal Physiology. W. B. Saunders & Co., Philadelphia, Pa. 75.

REESE, T., M. V. L. BENNETT, and W. FEDER. 1971. Cell to cell movement of peroxidase injected into the septate axon of crayfish. *Anat. Rec.* **169**:409.

ROJAS, E., and G. EHRENSTEIN. 1965. Voltage clamp experiments on axons with potassium as the only internal and external calcium ion. *J. Cell Comp. Physiol.* **66**:71–78. Supp. 2.

RUSHTON, W. A. H. 1945. Action potentials from the isolated nerve cord of the earthworm. *Proc. R. Soc. Lond. Ser. B Biol. Sci.* **132**:423–437.

STEPHENSON, J. 1930. The Oligochaeta. Reprint 1972. J. Cramer and H. K. Swann, editors. Vol. 92. Historiae Naturalis Classica Ediderunt. Stechant-Hafner Serv. Agency, New York.

STOUGH, H. 1926. Giant nerve fibers of the earthworm. *J. Comp. Neurol.* **40**:409–464.

SUBAK-SHARPE, J. H., R. R. BURK, and J. D. PITTS. 1969. Metabolic cooperation between biochemically marked mammalian cells in tissue culture. *J. Cell Sci.* **4**:353–367.

WEIDMANN, S. 1970. Electrical constants of trabecular muscle from mammalian heart. *J. Physiol. (Lond.).* **210**:1041–1054.

WEIDMANN, S. 1966. The diffusion of radiopotassium across intercalated discs of mammalian cardiac muscles. *J. Physiol. (Lond.).* **187**:323–342.

WEINGART, R. 1974. The permeability to TEA ions of the surface membrane and the intercalated discs of sheep and calf myocardium. *J. Physiol. (Lond.).* **240**:741–762.